Lubrication Properties of Protein Aggregate Dispersions in a Soft Contact

AGNIESZKA CHOJNICKA,*,†,‡ SASKIA DE JONG,†,§ CORNELUS G. DE KRUIF,‡,§ AND
RONALD W. VISSCHERS†,§

Wageningen Centre for Food Sciences, P.O. Box 557, 6700 AN Wageningen, The Netherlands,
Van't Hoff Laboratory for Physical and Colloid Chemistry, Debye Institute, Utrecht University,
Padualaan 8, 3584 CH Utrecht, The Netherlands, and Texture Department, NIZO Food Research,
Kernhemseweg 2, P.O. Box 20, 6710 BA Ede, The Netherlands

The lubrication, rheological, and molecular properties of two different protein aggregate dispersions were compared: globular aggregates of whey protein isolate (WPI) and fibrillar aggregates of ovalbumin from egg white. These dispersions are models for the lubricating fluid that is present between the tongue and the palate when consuming liquid or gelled products. To simulate oral conditions, a commercial tribometer was modified so that soft rubber surfaces could be used. This allowed us to measure friction at low contact pressures similar to those present between the tongue and palate. Clear correlations were observed between the measured friction coefficients and specific properties of the lubricating fluid such as protein concentration and aggregate size and shape. Furthermore, surface properties like elasticity, surface−surface interactions, and surface roughness had a significant effect on the friction under conditions that are relevant for texture perception. We conclude that in vitro measurements at low contact pressure provide valuable information for understanding and controlling food properties that modulate oral friction.

INTRODUCTION

Sensory perception of food is a complex process that involves all human senses (*1, 2*). Texture, or our perception of food structure, depends on (i) the composition and bulk rheological properties of the food, (ii) the properties of the oral surfaces that take part in the processing of the food, and (iii) the interactions between oral surface and food. Attributes such as creaminess, smoothness, and stickiness that describe the quality of the texture of food are easy to perceive but difficult to characterize physically (*3, 4*). The microstructure of proteins, fat, and possible networks of other ingredients will affect oral friction, and this will probably influence perception. Relations between texture sensation and microstructure of food have been demonstrated in some cases (*5–8*), but the relation between microstructure and tribological properties of food have not been studied extensively (*9–11*).

Frictional behavior of food systems in the gap between palate and tongue is of key relevance to the perceived texture of food. Friction between two sliding surfaces in general depends on (i) the properties of the lubricating substance separating the two surfaces (*12*), (ii) the force pressing the two surfaces together, and (iii) the roughness of the surfaces in contact. During consumption food acts as a lubricant substance, and therefore frictional forces during the oral processing will depend on the properties of the food material. More precisely, in this study the working hypothesis is that the force needed to slide the tongue over the palate depends on food properties and is relevant to the texture of food.

Typically, the oral regime is characterized by a mean low contact pressure and low traction speed during eating. The contact pressure in the mouth is estimated to be approximately 30 kPa (*13*). These low pressures cannot be easily achieved with standard tribometers. Steel−steel contacts under normal measuring conditions generate contact pressures in the GPa region. By modifying a tribometer to work with different rubber surfaces, we have been able to lower the contact pressure for our measurements to about 50–100 kPa. Oral friction also depends on the difference between sliding and rolling motions as well as on the shear rate. During mastication it is likely that different sliding and rolling motions are present between the tongue and palate depending on the consumed food. However, how this impacts on friction is not known since no data on in vivo or in vitro measurements are available. It has been shown

* To whom correspondence should be addressed at NIZO Food Research. Tel: +31-318-659-580. Fax: +31-318-650-400. E-mail: agnieszka.chojnicka@nizo.nl.
† Wageningen Centre for Food Sciences.
‡ Utrecht University.
§ NIZO Food Research.

Lubrication Properties of Protein Aggregate Dispersions

J. Agric. Food Chem., Vol. 56, No. 4, 2008 **1275**

that during mastication the shear rate applied in the mouth varies in between 1 and 1000 s^{-1} (*14*).

Roughness of oral surfaces also has a significant effect on the perceived texture of food. It is influenced by the amount of saliva and the amount and properties of the adhered food. Furthermore, the surface roughness can change as a result of abrasion of these layers during oral processing and may be affected by muscular contraction of the tongue muscles. Therefore, it seems particularly relevant to establish the relation between surface roughness and the amount of friction at contact pressure and traction speeds that are relevant for the oral regime (*5, 12, 15, 16*).

This paper focuses on the lubrication of protein aggregate dispersion and studies how protein ingredients modulate friction under conditions that are relevant for oral texture perception. These dispersions serve as a model for foods that are structured by a protein network. It was expected that the lubrication properties of the dispersions would vary with composition. Thus two different protein solutions were used: globular aggregates from whey protein isolate (WPI) and fibrillar aggregates from ovalbumin. The shape of the aggregates has a significant effect on the viscoelastic properties of the dispersions, and the aim of this work is to determine its influence on the lubrication properties. To our knowledge, this is the first time that a quantitative measurement is made of lubrication properties of protein aggregate dispersions between soft surfaces. Finally, it should be realized that consumption itself induces changes in the structure of the food (*15, 17*) or the oral tissue that can have an effect on the friction. These types of effects are not explicitly included in this study.

MATERIALS AND METHODS

Characteristics and Preparation of the Protein Aggregates. Lubricants studied in our experiments are dispersions of aggregates of ovalbumin and whey protein isolate (WPI). Ovalbumin was purchased from Sigma (albumin from chicken egg white, grade III, minimum 90% pure by agarose gel electrophoresis, crystallized and lyophilized, batch 074K7011). The second dispersion was made of Bipro, which is a whey protein mixture obtained from Davisco Foods International Inc. (La Sueur, MN). The WPI is mainly composed (based on dry weight) of 74% β-lactoglobulin (β-lg) and 13% α-lactalbumin (*18*).

Depending on the type of protein heated, different types of aggregate can be formed (*18*). In the case of heated WPI, globular protein aggregates are obtained, while ovalbumin aggregates are typically fibrillar in shape. The size and voluminosity of aggregates and thereby the viscosity can be controled by heating the solution at a specific concentration. The preparation of soluble WPI and ovalbumin aggregates was done according to Alting et al. and Weijers et al. (*19–22*).

Both proteins were dissolved in distilled water at ambient temperature to a concentration of 3%, 6%, and 9% for WPI and 2%, 3.5%, and 5.3% for ovalbumin. The pH was adjusted to 7, and in the case of ovalbumin the solutions were filtered through a 0.5 μm filter to remove any unsolubilized material prior to heating. After heating, the dispersions were cooled to room temperature in a water bath. The dispersions were stored at 4 °C and used within 4 days after preparation. According to Alting et al. (*21*) and Weijers et al. (*22*) the WPI forms aggregates with a diameter of 30−80 nm. The fibrillar aggregates formed during heating are 30−700 nm long. For different concentrations of the WPI protein aggregate dispersions the dynamic light scattering technique was used to verify that the hydrodynamic and gyration radii did not change after the MTM experiment.

Rheological Measurements. The viscosity data of the different protein aggregate dispersions were recorded at 21 and 31 °C using a standard rheometer (AR 2000; TA Instruments, Leatherhead, U.K.) with double concentric cylinder geometry. Flow deformation curves were obtained by measuring the viscosity as a function of increasing shear rate. The measurement consists of three steps (15 min each): a
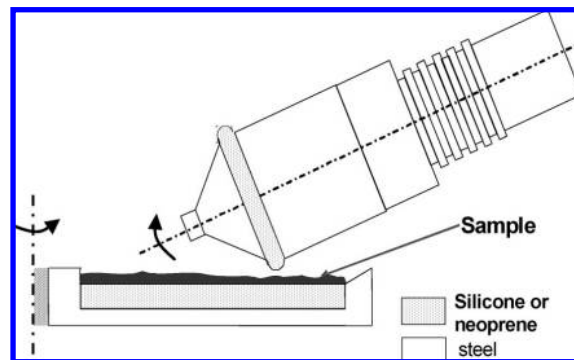

Figure 1. Schematic representation of the experimental setup. It consists of two essential parts: a neoprene ring and steel disk with an attached silicone or neoprene sheet on top of it. The dotted area represents the rubber surfaces that are in contact and are the source of friction.

Table 1. Comparison of the Pressure for Contact of Different Materials[a]

contact type	steel ball−steel	rubber ball−steel	rubber ball−rubber	rubber O-ring−rubber
pressure (Pa)	2.16×10^8	3.78×10^4	2.33×10^4	6.11×10^4

[a] All values were calculated using Hertz theory. In the case of the O-ring, the elliptical contact was taken into account.

conditioning step where the system is temperature equilibrated, followed by a continuous ramp step with the shear rate increased from 0.006 to 1000 s^{-1}. Finally, a reverse continuous ramp step was performed in order to check if there were any changes in the structure of the protein aggregates as a result of shearing. Each point was measured at a fixed shear rate with a duration time of 12–18 s. Brookfield oils (viscosity standard; Benelux Scientific, Scientific Instrument & Laboratory Equipment) with 10, 50, and 100 mPa were used to calibrate the equipment.

Tribological Measurements. A Mini Traction Machine (MTM) (PCS Instruments, London, U.K.) was used in the experiments to measure friction. Typically, a rotating steel disk and ball are used in this instrument as the two surfaces. The friction force arises from the ball−disk interaction at the applied speed. The rotating speed of the disk and the ball as well as the load can be adjusted using the instrument software. In order to study low contact pressure, the MTM was modified using compliant surfaces by introduction of a steel cylinder with an attached neoprene O-ring. In addition, a 3 mm silicone or neoprene sheet was fixed on top of the steel disk. To accommodate the layer of the rubber, the disk was modified (**Figure 1**). The flat surface and fixed position of the rubber on the steel disk was obtained by gluing it using Bison Kit transparent glue. Before experiments were performed all rubbers were cleaned with an ethanol, reverse osmosis water and dried with air. Since all of the results were reproducible and we have not noticed any changes after cleaning the rubbers, we assume that the cleaning procedure does not affect the measurements. The scatter points in the data are a good indication of their accuracy.

In this study the contact pressure was significantly lowered compared to the steel−steel contact. **Table 1** shows the calculated pressures for the different materials using $P = (W^{1/3}/\pi)[(4E^*)/(3R)]^{2/3}$, which is derived from the Hertz theory. W and R are the normal load and reduced radius, respectively. The contact modulus E^* is given in eq 4. Although the pressure obtained in this work is higher than the rubber−steel case, with our setup the friction can be investigated in the rubber−rubber contact. Moreover, the hard steel surface against the rubber causes cracking of the soft surface unlike in the case of the rubber−rubber contact. The latter due to the material flexibility causes weaker damage.

The rubber−rubber contact caused strong vibration of the ball−drive shaft at high speeds which could be only partially remedied by gluing the surface to the support. For this reason the upper limit of the speed had to be 600 or 750 mm/s. Due to technical reasons the data at speeds below 5 mm/s are very noisy, and therefore they are removed from

the figures. The slide roll ratio (SRR) is calculated using eq 1, where *U* is the mean tangential velocity of the ball and disk at the point of contact.

$$SRR = \frac{U_{disk} - U_{ball}}{U} \qquad (1)$$

All measurements were performed at a temperature of 21 or 31 °C (±1 °C) using the thermostat of the MTM. Sometimes wear of the material occurred during the measurements as a track became visible on the disk after repeated measurements. For this reason we limited the number of runs with the same surface and verified that wear did not result in significant changes over the period of the measurement.

Elasticity Measurements and Contact Pressure Calculation. The configuration where both the soft disk and the rubber ring were used made it possible to measure the relation between the friction coefficient and the entrainment speed at relatively low contact pressure. To estimate the contact pressure, the elasticity of the silicone and neoprene rubbers was measured. Young's modulus is calculated from the slope of the initial linear relation of the stress/strain curve. This relation was obtained using an Instron 5543 (Instron Int., Edegem, Belgium), where the rubber was placed between two parallel plates, which were pressed toward each other. Both rubbers were compressed at 1 mm/s and to 95% strain. The Young modulus for each rubber is a mean value obtained in eight independent measurements.

To calculate pressure in between two surfaces, the contact area has to be determined. In the case of the rubber ring the contact area has an elliptical shape and is described by two semiaxes given by Greenwood et al. (*23*):

$$a = \left(\frac{3k^2 \epsilon WR}{\pi E^*}\right)^{1/3}$$
$$b = \left(\frac{3\epsilon WR}{\pi k E^*}\right)^{1/3} \qquad (2)$$

The axis ratio $k = a/b$ can be approximated by $k \approx [1.0339(R_1/R_2)]^{0.636}$, while the elliptic integral $\epsilon \approx 1.0003 + 0.5968(R_2/R_1)$ (*23, 24*), where R_1 and R_2 are radii of the O-ring and its cross section, respectively. The reduced radius R is given by $(1/R_1 + 1/R_2)^{-1}$.

The contact pressure depends on the contact area between rubbers, the normal load applied, and the elasticity modulus of the materials. The elliptical contact area is given by

$$S = \pi ab \qquad (3)$$

The contact modulus using eq 2 is defined as

$$E^* = \left(\frac{1 - \nu_1^2}{E_1} + \frac{1 - \nu_2^2}{E_2}\right)^{-1} \qquad (4)$$

where the E_i and ν_i are the Young moduli and Poisson ratios of the two rubbers in contact. The Poisson ratio for rubbers is in good approximation 0.5.

Finally, the contact pressure is calculated:

$$P = W/S \qquad (5)$$

Contact Angle Measurements. To estimate the strength of the hydrophobic interactions between the protein aggregate dispersions and the different types of rubber disks, the contact angles between samples and the rubbers were measured. The contact angle measurement was done using a conventional goniometer (ERMA contact angle meter G-1). A symmetrical drop of around 0.5−0.7 cm radius was deposited on the surface material using a syringe with a constant solution volume of 10 μL. All rubbers were cleaned with an ethanol, reverse osmosis water and dried with air. The contact angles were collected visually at room temperature from both sides of the drop directly (within 1 min after the drop was applied). Reported contact angles are the average of 10 measurements.

Stereomicroscopy. Stereomicroscopy (Leica Microsystems MZ16 with optical zoom 16) was used to evaluate the surface of the rubbers. The objective lens used was a PL APO type with a numerical aperture of 0.20 and 1.7 μm resolving power. The image roughness was calculated using the method described in ref *25*.

RESULTS

Rheological Measurements. In order to understand the tribological data, we have determined the dynamic viscosity of the lubricants. The WPI and ovalbumin protein aggregate dispersions show non-Newtonian behavior: the viscosity decreased with shear rate, indicating that shear thinning occurred (**Figure 2**).

The viscosity increases with concentration and with volume factor. Ovalbumin protein aggregate dispersion had higher overall viscosities compared to WPI on a w/w basis, which is related to the fibrillar shape of the ovalbumin aggregates formed during incubation in the heater bath (*22*). Since the length of the fibrils formed is highly dependent on the protein concentration during heating (*19*), long fibrils and a high viscosity were observed near the critical gel concentration. Both the length of the aggregates and the viscosity decreased drastically when the concentration of the protein during heating is lowered. The changes in viscosity as a function of the concentration and the aggregate size were less significant in the case of WPI, which is known to form more globular-shaped aggregates during heating (*18*). It should be noted that no irreversible breakdown of aggregates was apparent in the rheological measurements.

Tribological Measurements. Figure 3 shows how the friction coefficient changed as a function of traction speed when different solutions (WPI and water) were present as a lubricant.
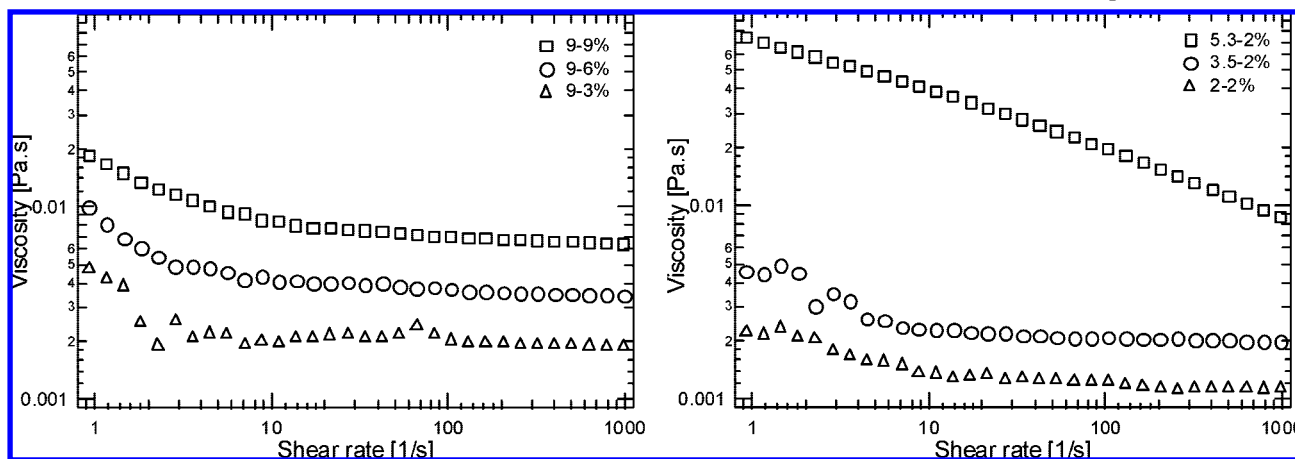

Figure 2. Viscosity data for WPI (left) and ovalbumin (right) protein aggregate dispersion. The effect of the protein concentration was shown for WPI where squares correspond to WPI 9%; this solution was diluted to 6% (circles) and to 3% (triangles). The effect of the aggregate size was shown for ovalbumin where all of the solutions were diluted to the same ending concentration with data points connected by the solid lines. Squares correspond to the ovalbumin 5.3–2%, circles to 3.5–2%, and triangles to ovalbumin 2%. Measurements were done at 31 °C.
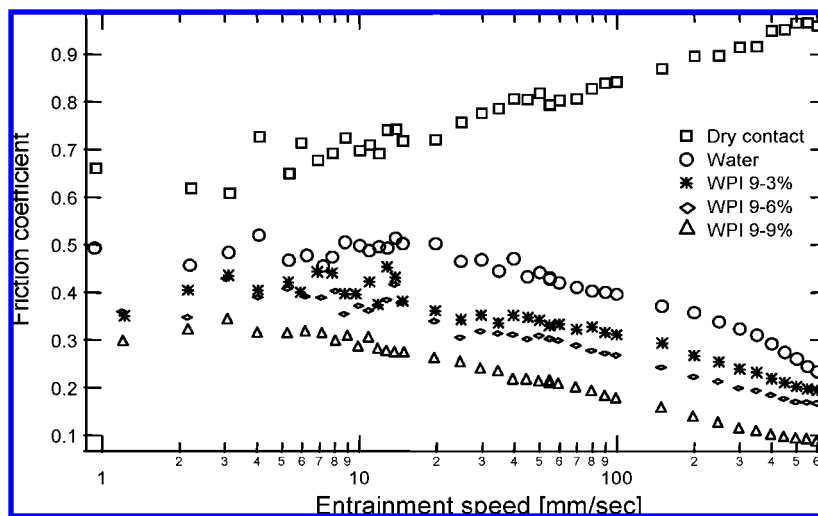
Lubrication Properties of Protein Aggregate Dispersions

J. Agric. Food Chem., Vol. 56, No. 4, 2008   **1277**

Figure 3. Stribeck curves for different lubricants: water (circles), WPI 9–3% (asterisk), WPI 9–6% (diamond), and WPI 9% (triangle). The effect of the protein concentration is noticed by diluting the solution with the same aggregate size to lower concentration. Squares correspond to the case where there is no lubricant present and the rubber ring and silicone sheets are in direct contact. Physical parameters: load 5N; $T = 30$ °C; SRR = 50%.
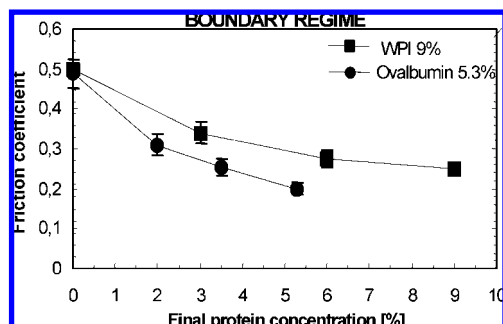

Figure 4. Friction coefficient in boundary lubrication regime (5−10 mm/ s) as a function of protein concentration for WPI and ovalbumin protein aggregate dispersions. The applied load was 5N for neoprene−silicone contact. For WPI a 9% solution was heated and after cooling diluted to the appropriate concentrations. For ovalbumin, the concentration during heating was 5.3%. The measurements were repeated for three times and averaged to give an averaged friction coefficient.

When there is no lubricant present, the friction coefficient increased linearly with increasing speed. When water is introduced as a lubricant, the friction coefficient at very low traction speed is about the same as for the dry contact. A mixed lubrication regime occurs at about 10–15 mm/s for the applied conditions. **Figure 3** demonstrates that when a small amount of WPI aggregates is present, the lubrication properties improved with respect to water. Both in the boundary as well as in the mixed regime friction is lower and depends on the concentration of the protein. **Figure 4** shows the concentration dependences of the friction coefficient in the boundary regime (5–10 mm/s) for both WPI and ovalbumin in a neoprene−silicone contact.

Higher concentrations for both types of protein aggregates yield lower friction coefficients in the boundary regime. The concentration dependence for both protein dispersions was similar and correlated with their viscosity. In most cases we observed the transition from boundary to mixed regime between 10–15 mm/s and slightly depended on concentration. In the boundary regime ovalbumin solutions had lower friction coefficients compared to WPI. For WPI, the boundary friction level decreased about 40% when the protein concentration was increased from 0 to 9% (see **Table 2**). For ovalbumin a 50% decrease was observed at a protein concentration of 5.3% relative to water. Also, the dependence of the friction coefficient

on the concentration was stronger for ovalbumin than for WPI in the mixed regime. We used a logarithmic function $\xi(U) = a_0 + a_1 \log U$ in order to be able to compare our results more quantitatively and to fit data in the mixed lubrication regime. Measurements of water were better represented by a linear function. **Table 2** summarizes the estimated boundary friction of the different protein aggregate dispersions and the fitted slope a_1 in the mixed regime as a function of WPI protein concentration.

The onset of the mixed regime appeared to shift to somewhat lower speeds when the protein concentration increases. The slope of the Stribeck curves in the mixed regime also depends on the protein concentration. At lower concentrations the friction in the mixed regime dropped faster with increasing speed.

To investigate the effect of aggregate size, the protein concentrations during heating were varied. Subsequently, the samples were diluted to equal concentrations (**Figure 5**), and friction measurements were made at different pressures. This is different from the data presented in **Figure 4**, where the concentration during heating was the same but the final protein concentrations were different.

Bigger aggregates cause a decrease of the friction coefficient in the boundary regime at equal protein concentrations for both types of protein aggregates. This is observed in the boundary regime and mixed regime, and it is more pronounced at low pressure (see below).

Figure 6 shows the relation between boundary friction and heating concentration for two different types of aggregates. The fact that the curves do not coincide is explained by the actual size of the aggregates. In case of WPI, aggregates have a globular shape, and sizes vary between 30 and 80 nm. Ovalbumin aggregates have a fibrillar shape, and sizes vary between ∼40 and 700 nm. The WPI and ovalbumin aggregates of small sizes (30 and 40 nm, respectively) show very similar friction coefficients (∼0.38). The trend is continued for larger sizes (80 and 100 nm), and friction decreases for both species to about 0.34 for ovalbumin and 0.3 for WPI. The largest ovalbumin aggregates also showed the lowest friction coefficient (∼0.2).

Interestingly, when the normal load is increased, the measured friction coefficient decreased for both types of protein aggregates as well as water. The differences in Stribeck curves for WPI protein aggregates dispersions obtained at 1N and 5N are shown in **Figure 5**. Similar behavior was observed for ovalbumin

Table 2. Friction Coefficient and Corresponding Speed Obtained in Boundary Lubrication Regime[a]

WPI concn (%)	upper limit, boundary plateau		slope a_1 in mixed regime		ovalbumin concn (%)	upper limit, boundary plateau	slope a_1 in mixed regime
	50% SRR	100% SRR	50% SRR	100% SRR		50% SRR	50% SRR
0	0.50, 10 mm/s	0.55, 20 mm/s	linear 0.42 ± 0.0025	-0.259 ± 0.0055	0	0.50, 10 mm/s	linear 0.42 ± 0.0025
3–3	0.40, 10 mm/s	0.45, 10 mm/s	-0.139 ± 0.0029	-0.180 ± 0.0034	2–2	0.35, 10 mm/s	-0.155 ± 0.00439
6–6	0.33, 15 mm/s	0.40, 15 mm/s	-0.129 ± 0.0032	-0.145 ± 0.0016	3.5–3.5	0.33, 16 mm/s	-0.103 ± 0.0021
9–9	0.33, 8 mm/s	0.35, 9 mm/s	-0.121 ± 0.002	-0.096 ± 0.0032	5.3–5.3	0.22, 20 mm/s	-0.087 ± 0.0031

[a] The slope results from fitting the Stribeck curve in the mixed regime. Notation: WPI 9–9% means that during the measurements the concentration of the protein aggregate dispersion was the same as in the heating procedure; WPI 9–3% means that the initial heated concentration of protein was 9%, and after cooling down the aggregate dispersion was diluted to 3% and measured.
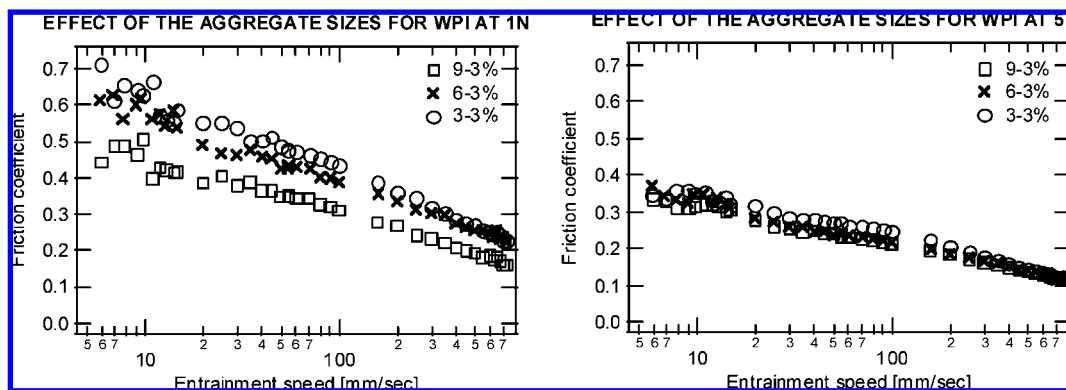

Figure 5. Influence of aggregate size on friction for WPI protein dispersion at 1N normal load (left) and 5N (right). The friction coefficient was measured in neoprene−silicone contact.
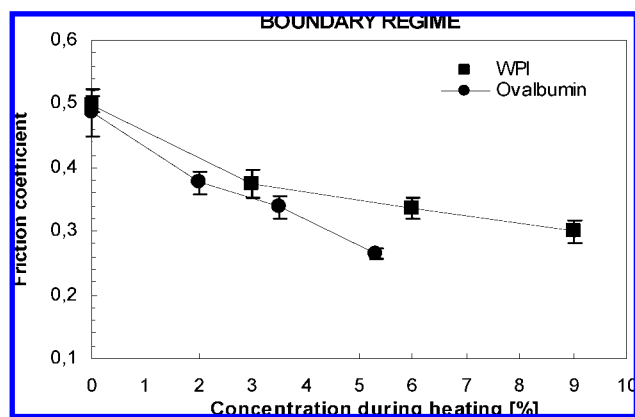

Figure 6. Friction coefficient in boundary lubrication regime (average value from 5 to 10 mm/s) as a function of aggregate size for WPI and ovalbumin protein aggregate solutions. The applied load was 5N. The measurements were repeated for three times and averaged to give an averaged friction coefficient.

aggregate dispersions. The results showed that in the case of 5N a lower friction coefficient is measured compared to the low load. According to a simple adhesion theory of friction, the friction coefficient is $\mu = F/W = S\tau/SP = \tau/P$, where τ is shear strength (26). Thus in the boundary and mixed regimes, where the surfaces are not separated, the friction coefficient decreases with increasing contact pressure. Indeed, the ratio of the friction coefficients determined at different normal loads is close to the ratio of the pressures corresponding to these loads. In the case of the smaller aggregates, however, that ratio shows deviation. The largest difference occurs at high speeds, where the lubrication starts to dominate. In the boundary regime, however, smaller aggregates seem to be less efficient lubricants at lower pressures. In the case of the largest aggregate (9–3% WPI) the ratio of the friction coefficients is 1.61 ± 0.09, while the corresponding pressure ratio is 1.71.

When changing the slide roll ratio from 50% to 100%, three

observations were made (see **Table 2**). First, the boundary friction value measured between 5 and 10 mm/s increased significantly. Second, the onset of the mixed regime occurred at slightly higher speeds, and, finally, the slope in the mixed regime became steeper (especially for the 3% and 6% protein concentrations). The explanation for this behavior can primarily be found in the deformability of the surface material. Soft material like rubber can deform due to the applied force, which results in increased contact area. This in turn causes higher values of boundary friction coefficients (shift upward). This effect is stronger when "more sliding" motion occurs. More sliding motion results in a later onset of the mixed regime, which implies a larger effect of surface asperities, which is in line with the increased mechanical interactions due to the sliding motion.

Influence of Surface Properties on the Friction Coefficient. In order to establish the relative importance of elasticity, surface−surface, surface−lubricant, and roughness on the friction coefficient, we compared friction for silicone and neoprene rubbers. **Figure 7** shows Stribeck curves for ovalbumin protein dispersion obtained for neoprene−neoprene contacts and neoprene−silicone contacts. Higher friction coefficients were obtained when neoprene was used for both surfaces, and also a larger influence of protein concentration on friction was observed in this case.

From the stress−strain relation Young's moduli were calculated to be $E_1 = 0.2$ MPa for the neoprene and $E_2 = 0.29$ MPa for the silicone disks. On the basis of these moduli the contact area and the contact pressure between two touching surfaces were calculated at 1N and 5N (**Table 3** and eqs 2−5). Indeed, the calculations show that the contact area for the soft neoprene−neoprene contact is about 10% larger compared to the neoprene−silicone contact. This results in a lower contact pressure and higher friction coefficient (**Figure 7**). The increase of the friction coefficient however, cannot be explained by the adhesion theory alone, since the ratio of the pressures is 1.1, while the ratio of the friction coefficients is above 2. This implies
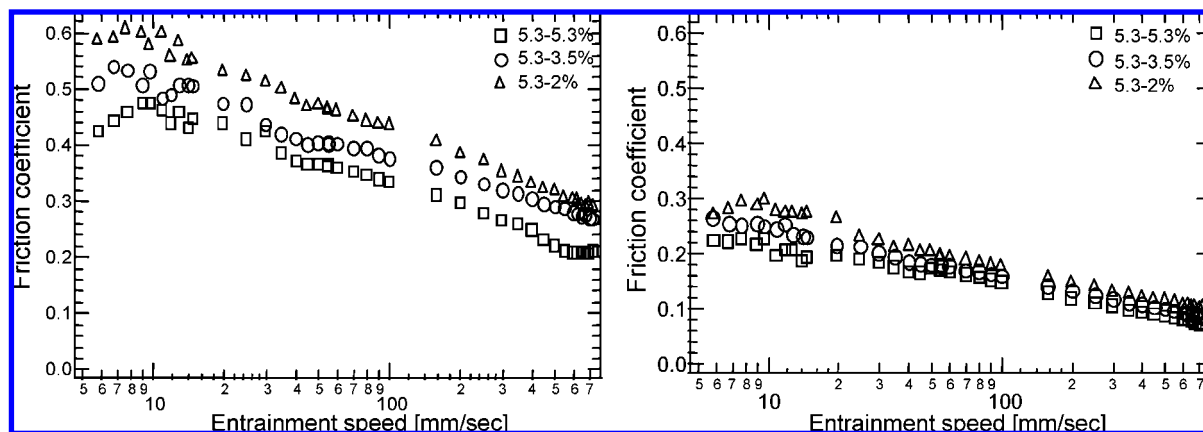
Lubrication Properties of Protein Aggregate Dispersions

J. Agric. Food Chem., Vol. 56, No. 4, 2008 **1279**

Figure 7. Stribeck curves for ovalbumin protein solution obtained for neoprene (left) and silicone (right) rubber at 5N of normal load.

Table 3. Contact Area and Contact Pressure for Neoprene−Silicone and Neoprene−Neoprene Rubbers Calculated for 1N and 5N Normal Load[a]

rubber	A (m^2), 1N	P (kPa), 1N	A (m^2), 5N	P (kPa), 5N
neoprene−silicone	1.64×10^{-5}	61.1	4.78×10^{-5}	104.6
neoprene−neoprene	1.83×10^{-5}	54.6	5.35×10^{-5}	93.4

[a] See eqs 2−5. The Poisson ratio was assumed to be 0.5 for both rubbers. The radius of the neoprene ring was measured to be $R = 9 \times 10^{-3}$ m while the cross-section radius was $r = 1 \times 10^{-3}$ m. From this the half-length and half-width of the contact area at $W = 5N$ were calculated to be $a_1 = 5.98 \times 10^{-3}$ m and $a_2 = 2.87 \times 10^{-3}$ m, respectively, while the half-length and half-width of the contact area at $W = 1N$ were calculated to be $a_1 = 3.48 \times 10^{-3}$ m and $a_2 = 1.67 \times 10^{-3}$ m, respectively.

Table 4. Contact Angle Measurements for Silicone and Neoprene Rubber[a]

rubber	water	WPI 3%	WPI 6%	WPI 9%
silicone	96.4 ± 2.9	102.2 ± 3.3	108.5 ± 3.8	109.2 ± 4.9
neoprene	79.5 ± 3.2	82.4 ± 4.7	88.6 ± 5.2	92.8 ± 6.3

[a] The readings were repeated for 10 times and averaged.

that at equal loads the observed difference probably originates from differences in surface properties and the adhesion which occurs at the region of contact, as well as on the surface roughness.

Contact angle measurements were made in order to investigate the wetting properties of the neoprene and silicone surfaces. This technique was used to characterize the affinity of water and aqueous solutions like our protein aggregate dispersions to coat the material. The results showed a smaller contact angle for the neoprene, indicating stronger attraction behavior of this rubber compared to the silicone (see **Table 4**).

The effect of wetting is more prominent for neoprene, meaning that the droplets become more spread on top of the neoprene surface than in the case of silicone. This is an indication of a more hydrophilic character of the neoprene. According to ref *27* using materials that facilitate formation of a water film would lead to a decrease of the observed friction. However, we generally observed a higher friction coefficient for neoprene−neoprene contacts compared to neoprene−silicone. This suggests that in our friction measurements not wetting but another effect dominates over the lubricant−surface interaction. Probably wetting and surface−lubricant interactions are more important at even lower pressures than we applied here.

In an alternative explanation for a system in which metal−rubber contacts were studied (*27*), it was suggested that less of the lubricant would flow into the contact zone when surfaces attract each other and friction will be higher at equal load (*28*). This appears to be more in line with our measurements since silicone is more hydrophobic than neoprene and more attraction will occur between the two neoprene surfaces. This would lead to less lubricant flowing into this contact, and indeed we observe a higher friction coefficient for the neoprene− neoprene contact compared to the neoprene−silicone contact at equal load, lubricant, and traction speed.

Surface roughness also differs between our silicone and neoprene material. It is likely that surface roughness has an effect on the pressure dependence since multiple contacts at high contact pressure can cause high friction for irregular surfaces (**Figure 8**). The surface roughness of the material was estimated according to a 2D Fourier transform method (*25*) of the rubber images obtained with a scanning microscope. The asperities of the neoprene ($R_q = 31 \pm 10$ μm) are about three times bigger compared to silicone ($R_q = 9 \pm 4$ μm). This difference in size of the asperities likely contributes significantly to the 3 times higher friction of neoprene compared to silicone when water is used as a lubricant. **Figure 7** shows that Stribeck curves obtained for different protein concentrations with a neoprene are more separated than with silicone, which might be due to the size of the asperities of the neoprene. Larger protein concentration can provide more material filling voids, which effectively lowers the surface roughness. In the case of silicone rubber that effect is weaker because asperities can be well leveled at lower concentrations.

Influence of Viscosity on the Friction Coefficient. In the full-film elastohydrodynamic regime the friction coefficient strongly depends on the viscosity of the lubricants as is predicted by elastohydrodynamic (EHL) theory. However, the effect of aggregate size and shape is more complicated. It should be realized that EHL theory (*29*) confirms that in the tribometer a very high shear rate is applied. We estimate that in the MTM even at very low velocities shear rates are already above 1000 s^{-1}. Thus our tribological measurements occur in the region where the shear rate dependence of the viscosity is probably not so strong. Therefore, we have made an analysis of the viscosity at the highest shear rates measured and the friction measurements at the high speed limit (~700 mm/s) (**Figure 9**).

Figure 9 demonstrates that WPI aggregates effectively lower the friction at much lower viscosities than ovalbumin aggregates. Next, it can be noticed that large ovalbumin aggregates are more effective at low concentration. This difference can be due to differences in shape or polymer−surface interactions.

Although in the mixed regime viscosity is not the main factor determining the friction coefficient, we have tried to estimate its contribution. In order to do this, we assumed a similar dependence
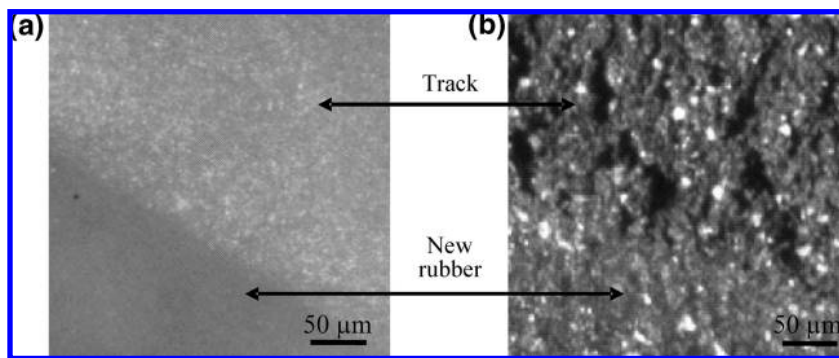
Figure 8. Scanning force microscope images obtained for silicone (**a**) and neoprene (**b**) rubber. The surface of the rubber before and after measurement is indicated.

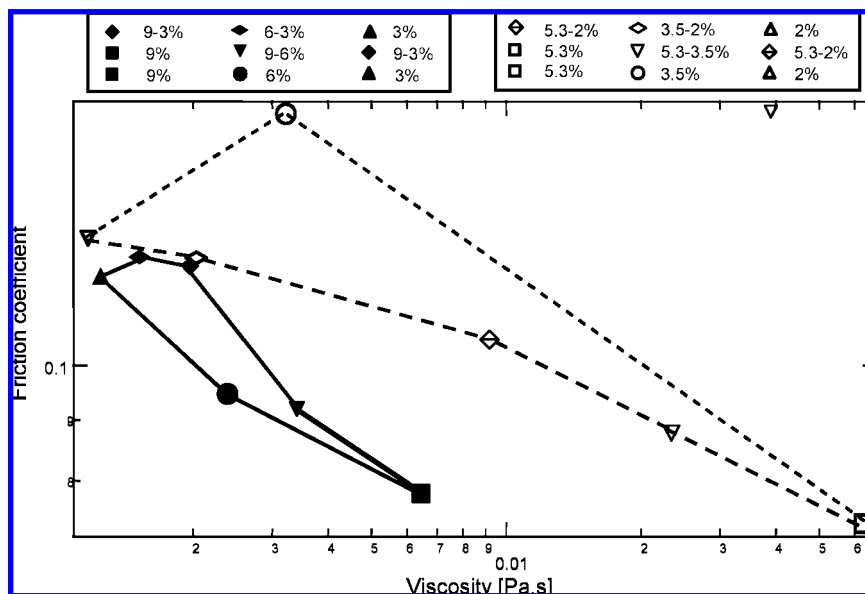**Figure 9.** Friction coefficient obtained at high mean speed as a function of viscosity measured at high shear rate ($\sim$1000 s^{-1}). The points correspond to data obtained for WPI and ovalbumin protein aggregate dispersion. Filled symbols connected with solid lines and open symbols connected with dashed lines correspond to data obtained for WPI and ovalbumin, respectively.
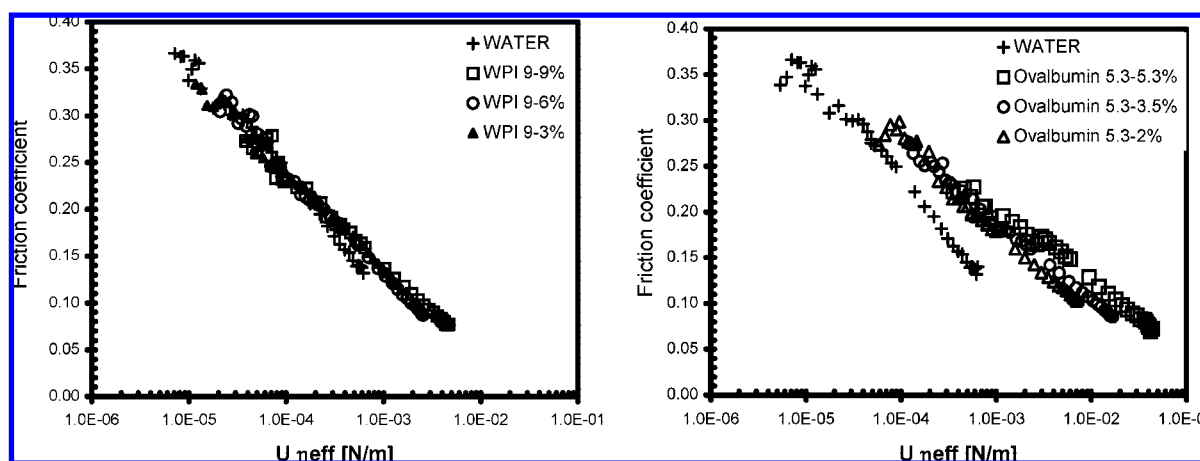

Figure 10. Friction coefficient versus effective viscosity (viscosity at shear rate of 1000 s^{-1}) for different concentrations of WPI (left) and ovalbumin (right). As a reference the water curve is also shown.

of the friction on the viscosity and speed, as predicted by EHL. We investigate the Stribeck curve as a function of the product of the speed and the effective viscosity. The latter was chosen to be the viscosity measured at shear rate 1000 s^{-1}. It should be noted that our assumption is based on full-film lubrication, while we have not fully entered that regime in our measurements. **Figure 10** shows

the friction coefficient versus the product of the speed and the effective viscosity for two different protein aggregate dispersions. The water curve is shown for comparison.

Different concentration curves of WPI collapse approximately to one line. This suggests that our initial assumption is valid and the decrease in the friction coefficient with concentration

Lubrication Properties of Protein Aggregate Dispersions

J. Agric. Food Chem., Vol. 56, No. 4, 2008 **1281**

is purely from the increase in viscosity of the system. In the case of ovalbumin, however, the concentration data do not collapse, meaning that other effects besides viscosity such as ordering of the fibrillar ovalbumin aggregates also have a significant contribution to the friction.

DISCUSSION

Lubrication Studied in a Soft Contact. Our results show that the concentration of protein aggregates as well as their size and shape in the lubricant significantly affects friction in a soft contact at relatively low pressure (50−100 kPa). A higher concentration of aggregates as well as larger particle size provides better lubrication. The boundary friction is effectively lowered by all of the protein dispersions with respect to water in a concentration-dependent manner. This shows that the number density of aggregates is more important at low speed. We speculate that the boundary regime is governed by the microproperties of the aggregate solutions, i.e., number of aggregates, their size, and sample−surface interactions like necking and failure or adhesion properties. The observed differences between ovalbumin and WPI aggregates may be explained by the fibrillar shape of the ovalbumin aggregates, allowing them to more effectively interact with a rough surface due to shear-induced ordering within the contact zone. Interestingly, Vicente et al. have observed that xanthan and guar gum solutions display opposite behavior in a rubber−metal contact, which was much smoother than ours. Asperity sizes of $R_q \approx$ 10 nm for the elastomer and $R_q \approx$ 800 nm in the case of steel (*28*) are over an order of magnitude smaller than the roughness present in this study (31 μm for neoprene and 9 μm for silicone). At low speeds the friction coefficient shows a very strong dependence on the concentration, while at high speeds the concentration becomes less important. At high speed it is the macroscopic properties that determine the flow of the lubricant and friction.

The friction cannot be predicted from the lubricant viscosity properties alone. At low contact pressure the effect of the slide roll ratio on friction is significant as is shown by our data. During oral processing, the tongue presses the food against the palate. Since the latter does not move, it is assumed that sliding movements dominate in the mouth. In practice, this process is more complex as far as the mandible movement; teeth squeezing and chewing play a role as well. In general, it is not easy to fully reproduce the process of consumption. Thus, to understand the oral condition better, the effect of changing the ratio of sliding and rolling motion has to be studied in more detail.

Figure 10 shows that the difference in the friction coefficient due to concentration is caused mainly by viscosity in the case of WPI. For ovalbumin dispersions the friction is most likely influenced also by other effects. These samples, however, exhibit non-Newtonian behavior, which may affect the choice of the effective viscosity. Moreover, the aggregate shape may also have some impact on the friction in the mixed regime. This effect, however, needs to be further investigated.

Deposition of protein material on the surfaces is probably an important issue that needs to be further studied. Higher protein concentration may cause a larger deposition of proteins, leading to formation of thicker adhered layers. Thus, when polymers adsorb on the material, a coating on the hydrophobic surface can occur, resulting in the reduction of the friction coefficient in the boundary regime. Also, deposition of material may explain the difference with the results for polysaccharide solutions as reported by Vicente et al. (*28*).

It is obvious that oral surfaces are elastic and tend to deform

under pressure. However, to what extend this contributes to changes in friction is not clear. For this reason, in this work two different rubber surfaces with different properties were used. Neoprene rubber is more elastic, which causes lower contact pressure for neoprene−neoprene configuration. The rougher neoprene surface shifts the onset of the mixed regime to higher entrainment speeds (up to 150 mm/s). In the highly concentrated ovalbumin solutions the onset of the mixed regime is again shifted to lower speeds, indicating that roughness is masked by high viscosity under this condition. We hypothesize that, for large enough asperities, the protein aggregate particles can be easily trapped in between them, thus effectively countering the roughness. This implies that adding protein aggregates induces a better lubrication on neoprene compared to silicone, which may explain the difference in concentration dependence observed in **Figure 7**.

Concluding Remarks. This study has shown that physical parameters such as normal load, elasticity, and slide roll ratio influence friction at conditions that are relevant for oral processing. At pressures and traction speeds relevant to oral conditions, as applied in our experiments, the amount of friction is influenced both by the bulk viscosity of the food in the mouth and by the roughness, elasticity, and surface−surface interactions of the oral tissue with the food. This suggests that it may possible to control oral perception by adjusting the friction either by changing concentration or by modulating surface roughness. Lubrication may be improved through the introduction of higher deformability of the surfaces and relatively high viscosity liquids. Surface roughness will counter this effect. The viscosity of the sample can be increased by raising the protein concentration, while the surface roughness on the other hand can be adjusted in the mouth by using material−surface interactions which especially have been noted for fibrillar ovalbumin aggregates. Clearly, both aspects need to be studied in more detail before they can be applied in real food systems.

ABBREVIATIONS USED

MTM, Mini Traction Machine; WPI, whey protein isolate; SRR, slide roll ratio; rms, root mean square; EHL, elastohydrodynamic theory; μ, friction coefficient; F, friction force (N); W, normal load (N); U_{disk}, speed of the disk (mm/s); U_{ball}, speed of the ball (mm/s); U, mean tangential velocity of the ball and disk (mm/s); R_1, radius of the neoprene ring; R_2, cross-section radius of the neoprene ring; a, b, semiaxes of the elliptical contact; k, elliptic integral; S, contact area between the rubber ring and rubber disks; ν_i, Poisson ratio of the rubbers; E_i, Young modulus of the rubbers (Pa); E^*, contact modulus of elasticity (Pa); P, contact pressure; η, viscosity (Pa·s); R_q, rms roughness of the rubbers (asperities); τ, shear strength.

LITERATURE CITED

(1) Tyle, P. *Acta Physiol.* **1993**, *84*, 111–118.
(2) Engelen, L.; de Wijk, R.; der Bilt, A.; Prinz, J. F.; Janssen, A. M.; Bosman, F. *Physiol. Behav.* **2005**, *86*, 111–117.

1282 *J. Agric. Food Chem.,* Vol. 56, No. 4, 2008

Chojnicka et al.

(3) Bogue, J.; Sorenson, D.; Delahunty, C. Determination of Consumers' Sensory Preferences for Full-fat and Reduced-fat Dairy Products, Agribusiness Discussion Paper No. 37, 2002.

(4) Phillips, L. O.; Mcgiff, M. L.; Barbano, D. M.; Lawless, H. T. The Influence of Fat on the Sensory Properties,Viscosity, and Color of Lowfat Milk. *J. Dairy Sci*. **1995**, *78*, 1258–1266.

(5) Malone, E.; Appelqvist, I. A. M.; Norton, I. T. *Food Hydrocolloids* **2003**, *17*, 763–773.

(6) Imai, E.; Saito, K.; Hatakeyama, M.; Hatae, K.; Shimada, A. *J. Texture Stud*. **1999**, *30*, 59–88.

(7) Langton, M.; Åström, A.; Hermansson, A. M. *Food Hydrocolloids* **1997**, *11*, 217–230.

(8) Lawless, H. T.; Heymann, H. *Sensory evaluation of food: principles and practices*; Chapman & Hall: New York, 1998; pp 379−405.

(9) Kokini, J. L. *J. Food Eng*. **1987**, *6*, 51–81.

(10) Giasson, S.; Israelachvili, J.; Yoshizawa, H. *J. Food Sci*. **1997**, *62*, 640–646.

(11) Luengo, G.; Tsuchiya, M.; Heuberger, M.; Israelachvili, J. *J. Food Sci*. **1997**, *62*, 767.

(12) Cassin, G.; Heinrich, E.; Spikes, H. A. *Tribol. Lett.* **2001**,*11*.

(13) Christiansen, J. B. **1979**, *5*, 335–337.

(14) Shama and Sherman (1973); Malone et al. (2003); Dickie and Kokini (1983).

(15) Malone, E.; Appelqvist, I. A. M.; Norton, I. T. *Food Hydrocolloids* **2003**, *17*, 775–784.

(16) Lee, S.; Heuberger, M.; Rousset, P.; Spencer, N. D. *Tribol. Lett*. **2004**, *16*, 239–249.

(17) de Wijk, R. A.; Prinz, J. F. *Food Qual. Prefer*. **2005**, *16*, 121–129.

(18) Alting, A. C.; Weijers, M.; de Hoog, E. H. A.; van de Pijpekamp, A. M.; Stuart, M. C.; Hamer, R. J.; de Kruif, K. G.; Visschers, R. W. *J. Agric. Food Chem*. **2004**,*52*, 623–631.

(19) Alting, A. C.; Hamer, R. J.; de Kruif, K. G.; Paques, M.; Visschers, R. W. *Food Hydrocolloids* **2003**, 1–11.

(20) Weijers, M.; Nicolai, T.; Visschers, R. W. *Macromolecules* **2002**, *35*, 4753–4762.

(21) Alting, A. C.; Hamer, R. J.; de Kruif, K. G.; Visschers, R. W. *J. Agric. Food Chem*. **2000**, *48*, 5001–5007.

(22) Weijers, M.; Barneveld, P. A.; Stuart, M. A. C.; Visschers, R. W. *Protein Sci*. **2003**, *12*, 2693–2703.

(23) Greenwood, J. A. Analysis of elliptical Hertzian contacts. *Tribol. Int*. **1997**, *30*, 235–237.

(24) Brewe, D. E.; Hamrock, B. J. Simplified solution for elliptical-contact deformation between two elastic solids. *ASME, J. Lub. Technol*. **1977**, *99*, 485–487.

(25) de Jong, S.; van de Velde, F. Charge density of polysaccharide controls microstructure and large deformation properties of mixed gels. *Food Hydrocolloids*,in press.

(26) Bowden, F. P.; Tabor, D. Friction, lubrication and wear: a survey of work during the last decade. *Br. J. Appl. Phys*. **1966**, *17*, 1521–1544.

(27) Ranc, H.; Elkhyat, C.; Servais, C.; Mac-Mary, S.; Launay, B.; Humbert, P. *Physicochem. Eng. Aspects* **2006**, *276*, 155–161.

(28) de Vicente, J.; Stokes, J. R.; Spikes, H. A. *Tribol. Int*. **2005**, *38*, 515–526.

(29) de Vincente, J.; Stokes, J. R.; Spikes, H. A. *Food Hydrocolloids* **2005**, 1–9.